# METHODS AND EXPERIMENTAL STUDY ON THE DETERMINATION OF FRICTION AND MECHANICAL PROPERTY PARAMETERS OF VARIOUS RICE SEED VARIETIES UNDER DIFFERENT CONDITIONS
/
# 不同状态下多种水稻种子摩擦与力学特性参数测定方法及试验研究

**Hanqing LI[1)], Shengnan LIU*[1)], Guangwei WU[2)], Bingxin YAN[2)], Lin LING[1,2)],**
[1)] College of Intelligent Manufacturing, Nanyang Institute of Technology / China
[2)] Research Center of Intelligent Equipment Technology, Beijing Academy of Agriculture and Forestry Sciences / China
[3)] College of Engineering Technology, Southwest University / China
*Tel: 0377-62232522; E-mail: LShengnan1210@163.com*
**Corresponding author: Shengnan LIU*
*DOI: https://doi.org/10.35633/inmateh-76-35*

***Keywords:*** *Rice, Multidimensional, Friction Characteristics, Mechanical Properties, Sowing Device*

## ABSTRACT
*Precision rice broadcasting technology plays a significant role in the mechanization of planting and yield enhancement, with seed friction and mechanical properties being critical factors in seeder design. In this study, experiments were conducted to evaluate the frictional and mechanical properties of different rice seed varieties. The results showed that higher seed moisture content led to reduced flowability and lower mechanical strength. When rice seeds underwent chitting treatment, their viability remained above 90% under external loads not exceeding 20 N or cutting lengths within 1.5 mm. This study provides a theoretical foundation and data support for the design and optimization of direct-seeding machinery, contributing to the advancement of rice direct-seeding technology and equipment.*

## 摘要
*水稻精准直播技术对种植机械化和产量提升意义重大，种子摩擦与力学特性是排种器设计的关键。因此，本研究对不同稻种的摩擦与力学特性进行实验。结果表明，种子含水率越高，流动性越差，力学强度越低。当种子处于露白处理后，外部载荷不超过 20 N 或切除长度不超过 1.5 mm 时，种子存活率均在 90%以上。本研究为水稻直播排种器设计优化提供了理论依据和数据支持，推动了水稻直播技术及装备发展。*

## INTRODUCTION
Rice, the staple food for over half of the global population, is critical for global food security *(Liberatore et al., 2025; Shang et al., 2024; Zhang et al., 2018*). However, traditional rice transplanting methods have become increasingly impractical due to rising labor costs and shifting rural demographics *(He et al., 2024; Qian et al., 2024*). In response, rice direct seeding technology has gained widespread adoption valued for its labor-saving, cost-effective, and high-efficiency characteristics (*Li et al., 2023a; Li et al., 2023b*). This approach involves mechanized direct seeding, eliminating the labor-intensive and resource-consuming aspects of traditional transplanting. Nevertheless, the precision of direct seeding remains constrained by the performance of seeders, which directly impacts seeding uniformity, seedling establishment rates, and overall field management costs *(Li et al., 2022; Liu et al., 2023*).

Accurate determination of seed mechanical and frictional characteristics is essential for developing theoretical models and defining simulation boundary conditions in seeder design *(Gao et al., 2022; He et al., 2022; Xing et al., 2018*). While traditional empirical trial-and-error approaches have been largely replaced by numerical simulations - such as those based on the Discrete Element Method (DEM) and Computational Fluid Dynamics (CFD) - the accuracy and completeness of material property parameters remain critical to simulation reliability. Previous studies have primarily focused on specific rice seed varieties or single physical states *(Dun et al., 2022; Wang et al., 2022a)*. Domestic researchers have conducted a series of studies on the characteristic parameters of rice seeds. The results indicated significant differences in the frictional and mechanical characteristic parameters among rice seeds of different varieties and types.

Currently, research methods are primarily focused on parameter calibration within EDEM software or rely on referencing and extending previous findings. However, existing studies still face limitations in both the scope of research objects and methodological innovation. Most research has concentrated on single rice varieties or seeds in the dry state *(Dong et al., 2022; Wang et al., 2022b)*. However, China's vast rice-growing regions span multiple climatic zones and involve diverse direct seeding practices - such as dry seeding, wet seeding, and film mulching - alongside a wide variety of rice types (including conventional, hybrid, and water-saving drought-resistant varieties). This complexity poses significant challenges to the applicability of existing parameter systems. In particular, the contact model parameters used in DEM simulations for rice seeds vary considerably depending on the seed's physical state. Relying on empirical or generalized parameters may result in design deviations in critical seeder components, ultimately reducing seeding efficiency and performance. Current methods for determining the mechanical and frictional properties of rice seeds are often limited to single varieties or seed states, and there is a lack of systematic studies encompassing multiple varieties and treatment conditions. Furthermore, the standardization of parameter acquisition methods remains inadequate, leading to poor data comparability across studies *(Li et al., 2021; Xing et al., 2021; Xing et al., 2020*).

To address these challenges, this study innovatively developed a multidimensional parameter determination system. The system encompassed seven conventional and three hybrid rice varieties, representing the primary direct-seeded rice types cultivated across China's major rice-growing regions *(Baral et al., 2021; Shun et al., 2020; Tang et al., 2021*). It simultaneously evaluated seeds in dry, soaked, and chitted states, and analyzed the effects of moisture content gradients on the mechanical and frictional properties of the seeds. This comprehensive approach enabled the establishment of accurate methods for determining the physical properties of rice seeds, offering strong theoretical and data support for the design and optimization of rice direct-seeding machinery. The findings lay a solid foundation for future theoretical modeling and virtual simulation studies, and ultimately contribute to the advancement of rice direct-seeding technology, improved mechanization, and enhanced national food security.

## MATERIALS AND METHODS

### *Experimental Materials*

This study selected 7 conventional rice varieties (Suigeng 27, Longjing 31, Nangeng 9108, Huanghuazhan, Xiangzaoxian 45, Longken 2021, Nongken 58) and 3 hybrid rice varieties (Jingliangyouhuazhan, Jingliangyou 534, Longliangyouhuazhan) as experimental materials based on dimensions such as planting areas, promotion areas, and farmer preferences. For ease of data compilation, the 10 different rice varieties were represented as $M_i$, where $M_1$ represented Suigeng 27, $M_2$ represented Longjing 31, $M_3$ represented Nangeng 9108, $M_4$ represented Huanghuazhan, $M_5$ represented Xiangzaoxian 45, $M6$ represented Longken 2021, $M_7$ represented Nongken 58, $M_8$ represented Jingliangyouhuazhan, $M_9$ represented Jingliangyou 534, and $M_{10}$ represented Longliangyouhuazhan. Different states of rice varieties were represented as $G_i$, where $G_1$ represented untreated and $G_2$ represented treated with exposure.

### *Experimental Methods*

The friction and mechanical properties of rice seeds could serve as a basis for analyzing the complex motion mechanisms such as friction and rolling between the seed population inside the seeder and between seeds and working components. This effectively revealed the operational mechanisms for precise seeding in rice precision hole direct seeding seeders.

### *Static Friction Coefficient*

The static friction coefficient was crucial for assessing a material's scattering performance. In this study, the inclined plane method was utilized to measure the static friction coefficient of rice seeds. The procedure involved placing the material on an inclined plane in contact with the rice seeds and gradually tilting it until sliding occurred. High-speed photography captured the angle between the inclined and horizontal planes at the onset of sliding. The tangent of this angle represented the static friction coefficient. Measurements were conducted using a custom-built device, depicted in Figure 1.

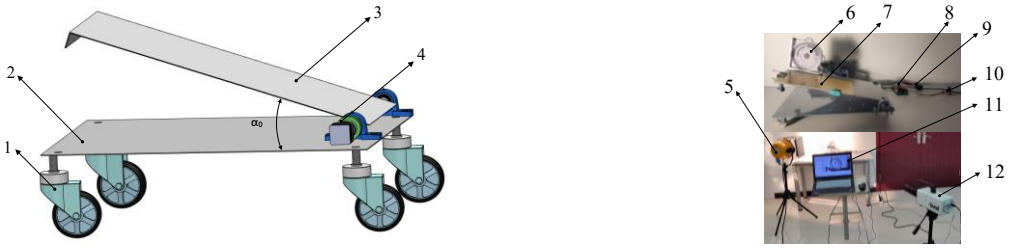


**Fig.1 - Static friction coefficient measuring device**

*(1) Supporting Wheel; (2) Base Plate; (3) Inclined Plane; (4) Drive Motor; (5) Supplementary Lighting Device; (6) Angle Measurement Instrument; (7) Contact Material; (8) Microcontroller; (9) Start-Stop Button; (10) Speed Controller; (11) Computer Terminal; (12) High-Speed Photography Device*

Different contact materials could be installed on the inclined plane, and when rice seeds came into contact with different materials, simply placing the respective material on the inclined plane was sufficient. During measurement, 100 grains of each of 10 randomly selected rice varieties in different states were placed on different contact materials on the inclined plane. The start-stop button was then activated to slowly raise the inclined plane. The computer terminal recorded the angles between different rice varieties in different states and different contact materials, providing a theoretical basis for subsequent simulation and theoretical analysis studies. The formula for calculating the static friction coefficient was shown in Equation 1.

$$\mu_1 = \tan\alpha_0 \tag{1}$$

where: $\mu_1$ is the static friction coefficient, and $\alpha_0$ is the angle between the contact surface and the horizontal plane (°).

***Coefficient of Dynamic Friction***

When the rice seeds moved on the inclined plane at different angles of inclination $\alpha_0$, the experiment involved capturing the coordinates $(x_{n-1}, y_{n-1})$, $(x_n, y_n)$, and $(x_{n+1}, y_{n+1})$ corresponding to frames $n-1$, $n$, and $n+1$ using a high-speed photography device, with each frame interval was $t_0$, as illustrated in Figure 2.

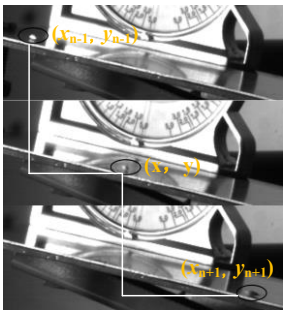


**Fig.** Error! No text of specified style in document. **- Rice seed coordinate point measurement**

Based on the coordinates measured for the rice seeds, the instantaneous velocity $v_0$ of the rice seeds at frame n could be calculated. The formula for calculating the instantaneous velocity $v_0$ was shown in Equation 2.

$$v_0 = \frac{\sqrt{(x_n - x_{n-1})^2 + (y_n - y_{n-1})^2} + \sqrt{(x_{n+1} - x_n)^2 + (y_{n+1} - y_n)^2}}{2t_0} \tag{2}$$

By measuring the instantaneous velocity of the rice seeds at time point $n$, it was possible to further calculate the rice seeds' instantaneous kinetic energy at that moment. Simultaneously, by using the specific coordinates of the rice seeds at time point n, the total distance traveled by the rice seeds along the inclined plane since the release could be determined. Based on this distance, it was then possible to estimate the proportion of energy loss due to frictional forces during the movement of the rice seeds on the inclined plane to the total energy.

The formula for calculating this proportion was shown in Equation 3.

$$C_0 = \frac{W_f}{U_0} = \frac{k_0 mg\cos\alpha_0 \cdot L_0}{mgL_0\sin\alpha_0} = k_0\cot\alpha_0 \tag{3}$$

where:

$C_0$ represents the proportion of lost energy to total energy; $W_f$ denotes the work done by frictional force, (J); $U_0$ stands for gravitational potential energy, (J); $k_0$ represents the coefficient of dynamic friction; $m$ is the mass of the grains, (g); $g$ is the acceleration due to gravity, (m/s²); $L_0$ is the travel distance of the rice seeds on the inclined plane, (m).

From Equation 3, it could be observed that the proportion of lost energy to total energy was linearly related to the cotangent of the angle, with the coefficient of dynamic friction as the correlation factor. Therefore, by varying the angle $\alpha_0$ between the inclined plane and the horizontal plane, it was possible to calculate the proportion of different lost energy to total energy. Subsequently, by performing a linear regression, the relationship between $C_0$ and $\cot\alpha_0$ could be fitted, with the slope of the fitted line represented the coefficient of dynamic friction.

***Elastic Modulus***

The experiment utilized a TMS food physical performance analyzer from FTC, as shown in Figure 3, to evaluate the elastic modulus, shear modulus, and Poisson's ratio of rice seeds. The sensor had a measurement range of 0–2000 N, with an accuracy of 0.015% and a data acquisition frequency of 10 Hz. To reduce the risk of cracking in white rice seeds during testing, the samples were prepared by trimming their axial ends. The height, width, and thickness of each sample were measured to calculate the cross-sectional area. The elastic modulus is a critical parameter that reflects the seeds' resistance to deformation under external forces. This mechanical property is essential for evaluating seed stability within seeders and their capacity to withstand pressure and impact during handling and movement in direct-seeding equipment.

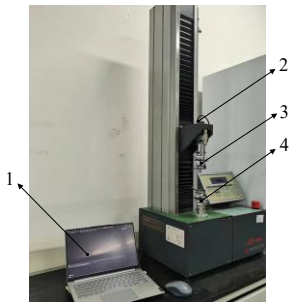


**Fig. 3 - Mechanical properties test instrument**

*(1) Data Acquisition Device; (2) Sensor; (3) Compression Probe; (4) Baseplate*

In the compression experiments, the elastic modulus of rice seeds was determined as the ratio of stress to strain. When a force was applied to a sample with a known cross-sectional area and initial length, the sample underwent deformation. Within the elastic range, stress was defined as the applied force per unit area, while strain was defined as the deformation per unit length. By measuring these two parameters, the elastic modulus was calculated according to Equation (4).

$$\begin{cases} E_1 = \frac{\sigma_0}{\varepsilon_0} \\ \sigma_0 = \frac{F_0}{A_0} \\ \varepsilon_0 = \frac{\Delta L_1}{L_1} \end{cases} \quad (4)$$

where:

$E_1$ is the elastic modulus of the rice seed, (MPa); $\sigma_0$ is the stress acting on the rice seed, (MPa); $\varepsilon_0$ is the strain of the rice seed; $F_0$ is the force applied axially to the rice seed, (N); $A_0$ is the cross-sectional area of the rice seed, in square meters ($m^2$); $\triangle L_1$ is the length of the cross-section, (m); and $L_1$ is the deformation of the cross-section, (m).

To measure the elastic modulus of rice seeds, 10 grains were randomly selected from various samples and the moisture content for the white rice treatment group was adjusted. During the compression test, the compression probe was configured to move at 20 mm/min, with a test speed of 1 mm/min and a return speed of 50 mm/min. The maximum testing distance was set to 60% of the specimen's length.

***Shear Modulus***

The preparation of test samples and the experimental procedure followed the same methodology used for measuring the elastic modulus, with calculations provided in Equation (5). Prior to the experiment, the following parameters were configured: the probe's moving speed was set to 20 mm/min, the test speed to 1 mm/min, and the initial pressure to 0.1 N. The maximum testing distance was set to 120% of the specimen's original length, and during the return phase, the return speed was adjusted to 50 mm/min.

$$\begin{cases} E_2 = \frac{\tau_0}{\zeta_0} \\ \tau_0 = \frac{F_1}{A_1} \\ \zeta_0 = \frac{\Delta L_2}{L_2} \end{cases} \quad (5)$$

where:

$E_2$ is the shear modulus of the rice seed, (MPa); $\tau_0$ is the shear stress acting on the rice seed, (MPa); $\zeta_0$ is the shear strain of the rice seed; $F_1$ is the force applied to the cross-section of the rice seed, (N); $A_1$ is the area on which the force is applied on the upper surface of the rice seed, (m$^2$); $\triangle L_2$ is the distance moved on the upper surface, (m); and $L_2$ is the deformation of the upper surface, (m).

***Coefficient of Restitution***

A coefficient of restitution of 1, 0, and less than 1 respectively indicated that the collision of particles was perfectly elastic, perfectly inelastic, and partially inelastic. This signifies that particles could fully recover to their original state, particles could not recover to their original state, and there was energy loss in particles after collision. The calculation formula for the coefficient of restitution is shown in Equation 6.

$$e^2 = \frac{E_3}{E_4} \quad (6)$$

where:

$e$ is the coefficient of restitution; $E_3$ is the energy after the collision, measured in joules, (J); and $E_4$ is the energy before the collision, (J).

Using the energy physics definition of the coefficient of restitution, a measurement model was established as depicted in Figure 4.

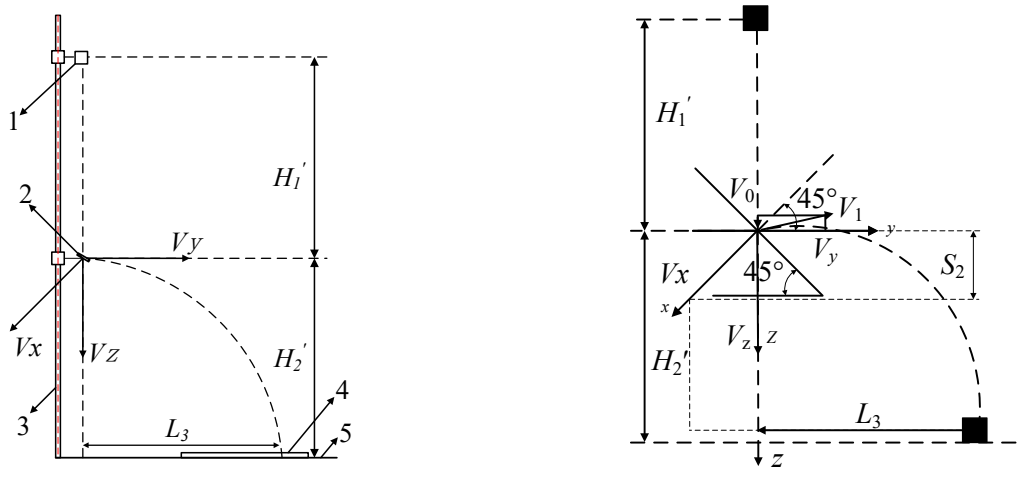


**(a)** **(b)**

**Fig. 4 - Measurement principle of collision recovery coefficient**

*(1) Seed Drop Point; (2) Inclined Plane (45°); (3) Support Stand; (4) Coordinate Collection Plate; (5) Support Plate; (a) Measurement Principle; (b) Velocity Decomposition*

In this model, a seed underwent free fall from a fixed height with an initial velocity of zero. Upon colliding with the contact material, the seed's velocity was decomposed into the x, y, and z axes. The collision height was set to a constant value. Due to the seed's geometric shape and instantaneous friction during the collision, it experienced displacement along the x and y axes post-collision. High-speed photography captured the entire sequence from collision to landing on the collection plate. By varying the contact test plate, the coefficient of restitution between the rice seed and different contact materials under various conditions could be determined.

One hundred rice seeds were individually dropped from the seeding point with zero initial velocity. During the descent, the seeds first encountered a 45° inclined plate, and then followed a projectile motion to land on the coordinate collection plate. To prevent the seeds from sliding on the coordinate collection plate, a layer of oil was applied to its surface. When the test rice seeds fell onto the coordinate collection plate at the bottom, the coordinate points of each experimental sample were statistically analyzed. Based on this, IBM SPSS software was used to post-process the data of each variety to determine the center coordinates of the seeds and calculate the distance from the center point to the origin. The distance from the center point to the origin satisfies the Pythagorean theorem with the horizontal and tangential deviations of the seeds. During the experiment, a high-speed camera was used to measure the average time taken for the seeds to collide and fall. The formula for calculating the coefficient of restitution is shown in Equation 7.

$$e = \sqrt{\frac{E_3}{E_4}} = \sqrt{\frac{V_x^2+V_y^2+V_z^2}{2gH_1}} = \sqrt{\frac{S_2^2+L_3^2+\left(H_2-\frac{1}{2}gT_1{}^2\right)^2}{2gH_1T_1{}^2}} = \sqrt{\frac{D_1^2+\left(H_2-\frac{1}{2}gT_1{}^2\right)^2}{2gH_1T_1{}^2}} \quad (7)$$

where:

$V_x$ is the velocity component along the x-axis of the rice seed after collision, (m/s); $V_y$ is the velocity component along the y-axis of the rice seed after collision, (m/s); $V_z$ is the velocity component along the z-axis of the rice seed after collision, (m/s); $g$ is the acceleration due to gravity for the rice seed, (9.8 m/s²); $S_2$ is the tangential deviation distance of the rice seed's motion after collision, (m); $L_3$ is the horizontal deviation distance of the rice seed's motion after collision, (m); $D_1$ is the distance from the center to the origin, (m); and $T_1$ is the average time taken for the rice seed to fall after collision, (s).

***External Load and Survival Characteristics***

Initially, 10 rice seed varieties under different conditions were selected, with each variety divided into 3 groups of 50 seeds. The moisture content for the white exposure treatment group was adjusted accordingly. Seeds that met sowing criteria were secured in a prone position on the base of a mechanical testing instrument. A rigid probe head served as the flat probe, descended at 2 mm/min and applied a load started from 0 N, increased by 5 N per test group along the seed embryo's thickness. Afterwards, samples were placed in planting pots within a controlled environment at 20°C to 25°C with appropriate lighting, as shown in Figure 5.

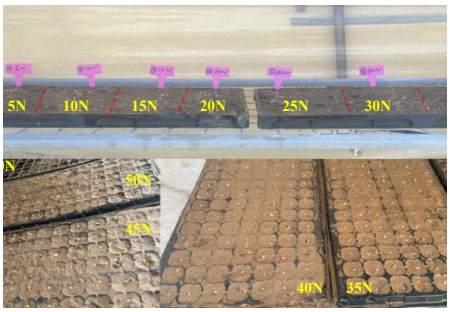


**Fig. 5 - External static load and survival test**

The non-white exposure group was watered twice daily to ensure thorough soil saturation. After germination and stabilization, the growth continuation percentage post-load was calculated for each sample group, based on consistent data over three consecutive days.

***Cutting and Seedling Characteristics***

Ten different varieties of rice seeds in different conditions were selected for this study. Specifically, three groups of each variety, with 50 rice seeds in each group, were chosen as experimental samples. The moisture content of the rice seeds in the white exposure treatment group was adjusted accordingly. Each group of experimental samples has the rice seeds cut along the embryonic axis, with the embryo length being approximately 3 mm. Therefore, the difference in embryo length cut each time is 0.5 mm. The rice seeds after cutting were then used for sowing experiments to evaluate their ability to continue surviving based on their germination status. The experimental process and methods were the same as those in the External Load and Survival Characteristics test. By analyzing the experimental data, the relationship between cutting length and survival rate was determined.

## RESULTS AND ANALYSIS

### *Experiment Results and Analysis of Static Friction Coefficient*

ABS resin was chosen as a contact material and various materials were affixed to an inclined surface on a custom static friction coefficient measurement device. Seed boards were created by attaching rice seeds to resin boards, simulating seed-to-seed contact. A brush board was made by attaching brush material to resin boards to simulate seed-to-brush contact, reflecting common seeding device configurations. This setup enabled separate measurement of static friction coefficients between rice seeds, and between seeds and ABS plastic or brush materials. High-speed photography captured the angle at which the inclined surface was gradually raised. These angle values were substituted into a formula to calculate the static friction coefficients. The experimental results were detailed in Table 1.

**Table 1**

**Static friction coefficient test results**

| Experiment Rice Seeds | Contact Materials | | | Experiment Rice Seeds | Contact Materials | | |
|---|---|---|---|---|---|---|---|
| | Rice Seeds | ABS | Brushes | | Rice Seeds | ABS | Brushes |
| $G_1$-$M_1$ | 0.36 | 0.28 | 0.32 | $G_2$-$M_1$ | 0.54 | 0.42 | 0.46 |
| $G_1$-$M_2$ | 0.39 | 0.30 | 0.34 | $G_2$-$M_2$ | 0.64 | 0.48 | 0.52 |
| $G_1$-$M_3$ | 0.41 | 0.29 | 0.33 | $G_2$-$M_3$ | 0.61 | 0.46 | 0.50 |
| $G_1$-$M_4$ | 0.36 | 0.23 | 0.26 | $G_2$-$M_4$ | 0.52 | 0.37 | 0.41 |
| $G_1$-$M_5$ | 0.31 | 0.20 | 0.24 | $G_2$-$M_5$ | 0.54 | 0.39 | 0.42 |
| $G_1$-$M_6$ | 0.34 | 0.23 | 0.26 | $G_2$-$M_6$ | 0.59 | 0.45 | 0.49 |
| $G_1$-$M_7$ | 0.37 | 0.25 | 0.29 | $G_2$-$M_7$ | 0.55 | 0.40 | 0.44 |
| $G_1$-$M_8$ | 0.33 | 0.22 | 0.25 | $G_2$-$M_8$ | 0.59 | 0.43 | 0.48 |
| $G_1$-$M_9$ | 0.37 | 0.23 | 0.27 | $G_2$-$M_9$ | 0.63 | 0.47 | 0.51 |
| $G_1$-$M_{10}$ | 0.35 | 0.21 | 0.25 | $G_2$-$M_{10}$ | 0.61 | 0.44 | 0.48 |

The analysis indicated that the rice seed variety had minimal impact on the static friction coefficient, while the moisture content had a significant effect. For dry seeds, the static friction coefficients between seeds, between seeds and ABS plastic, and between seeds and a brush were in the ranges of 0.31 to 0.41, 0.20 to 0.30, and 0.24 to 0.34, respectively. After chitting treatment, these values increased to 0.52–0.64, 0.37–0.48, and 0.41–0.52, respectively. This is because the increased moisture enhanced the adhesion forces, thereby raised the static friction coefficient and reduced the flowability. Further analysis reveals that at the same moisture level, the friction between rice seeds was higher than that between seeds and ABS plastic, suggesting that the surface of rice seeds was rougher and that the flowability on the ABS plastic surface was better.

### *Experiment Results and Analysis of Dynamic Friction Coefficient*

Rice seeds were placed at a certain height on an inclined plane with a certain angle to the horizontal plane and were initially at rest before sliding along the incline. By analyzing high-speed photography videos, the coordinates of the seeds in each frame could be obtained, with the experimental data extracted a time interval of 0.001 s between two frames. The experiment involved selecting five incline angles ranged from 10° to 50°, with 10 seeds of each variety tested for each angle and the average value taken. The experimental results were shown in Figure 6.

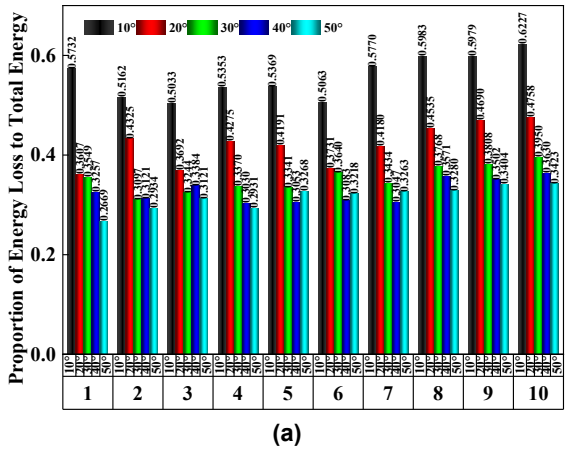


(a)

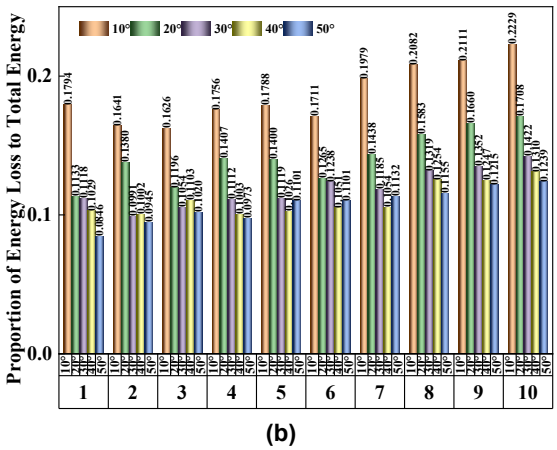


(b)

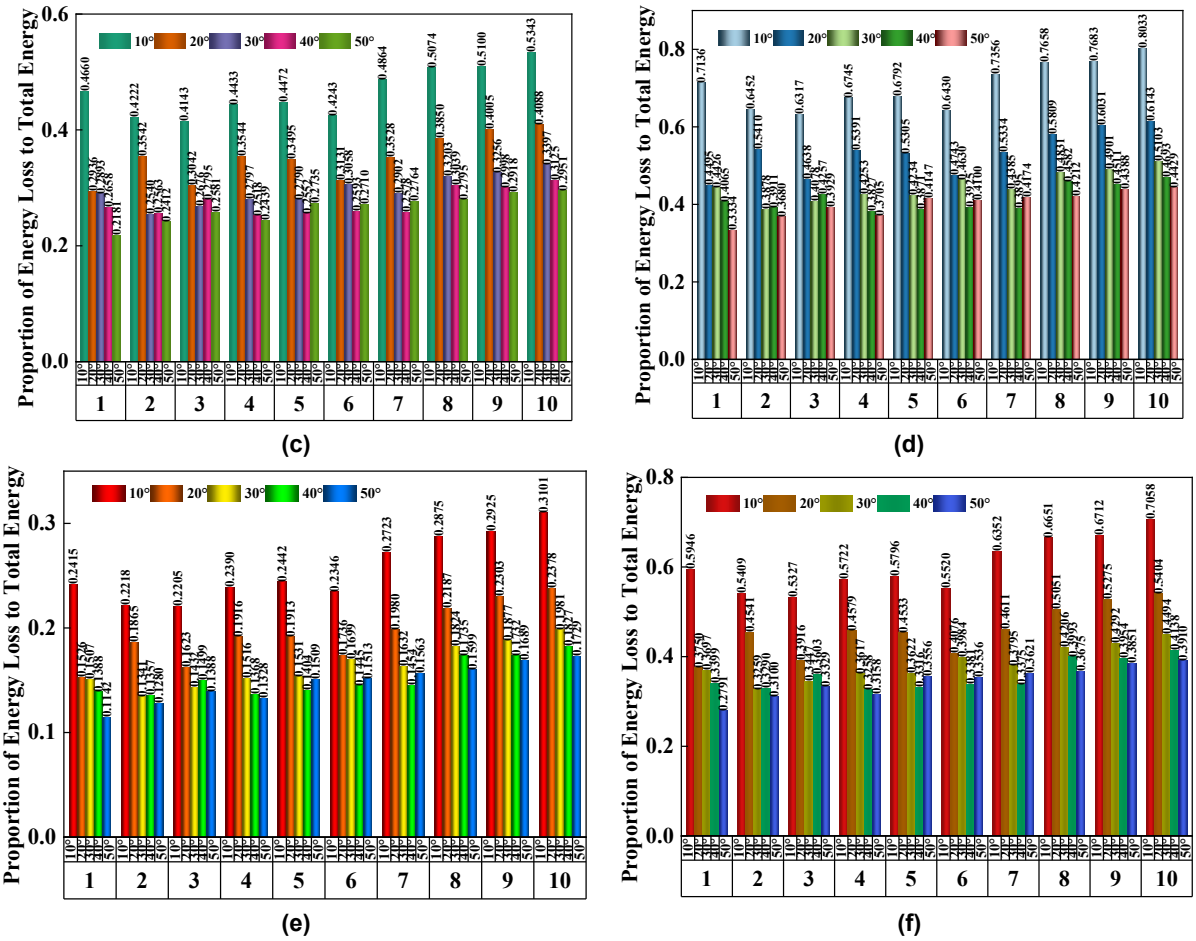


**Fig. 6 - Dynamic friction coefficient test results**

*(a) $G_1$ Rice Variety - $G_1$ Rice Variety (b) $G_1$ Rice Variety - ABS Material (c) $G_1$ Rice Variety - Bristle Brush*
*(d) $G_2$ Rice Variety - $G_2$ Rice Variety (e) $G_2$ Rice Variety - ABS Material (f) $G_2$ Rice Variety - Bristle Brush*

The results indicated that whitening treatment increased the energy loss proportion in rice varieties, suggested greater energy dissipation on the contact surface and a higher friction coefficient. As the angle increased, energy loss proportion decreased due to the conversion of gravitational potential energy into kinetic energy and frictional heat, with shorter incline travel time reducing energy loss. Among different conditions, energy loss was greatest between rice varieties, followed by rice varieties with bristle brushes, and lowest with ABS materials, highlighting better flowability on ABS. Linear fitting of the energy loss proportion ($C_0$) against cot $\alpha_0$ for each contact material yielded the dynamic friction coefficients $k_0$, as shown in Table 2.

**Table 2**

**Coefficient of dynamic friction between different kinds of rice and different materials**

| Experiment Rice Seeds | Materials | | | Experiment Rice Seeds | Materials | | |
|---|---|---|---|---|---|---|---|
| | Rice Seeds | ABS | Brushes | | Rice Seeds | ABS | Brushes |
| $G_1$-$M_1$ | 0.0601 | 0.0181 | 0.0427 | $G_2$-$M_1$ | 0.0724 | 0.0242 | 0.0601 |
| $G_1$-$M_2$ | 0.0494 | 0.0151 | 0.0391 | $G_2$-$M_2$ | 0.0599 | 0.0203 | 0.0499 |
| $G_1$-$M_3$ | 0.0411 | 0.0124 | 0.0321 | $G_2$-$M_3$ | 0.0490 | 0.0168 | 0.0411 |
| $G_1$-$M_4$ | 0.0547 | 0.0167 | 0.0472 | $G_2$-$M_4$ | 0.0648 | 0.0227 | 0.0547 |
| $G_1$-$M_5$ | 0.0515 | 0.0158 | 0.0398 | $G_2$-$M_5$ | 0.0607 | 0.0215 | 0.0515 |
| $G_1$-$M_6$ | 0.0426 | 0.0131 | 0.0329 | $G_2$-$M_6$ | 0.0501 | 0.0179 | 0.0426 |
| $G_1$-$M_7$ | 0.0615 | 0.0191 | 0.0472 | $G_2$-$M_7$ | 0.0716 | 0.0262 | 0.0615 |
| $G_1$-$M_8$ | 0.0613 | 0.0193 | 0.0496 | $G_2$-$M_8$ | 0.0709 | 0.0263 | 0.0612 |
| $G_1$-$M_9$ | 0.0611 | 0.0192 | 0.0466 | $G_2$-$M_9$ | 0.0703 | 0.0264 | 0.0611 |
| $G_1$-$M_{10}$ | 0.0657 | 0.0207 | 0.0499 | $G_2$-$M_{10}$ | 0.0751 | 0.0286 | 0.0657 |

The results showed that in dry conditions, the average dynamic friction coefficients were 0.0411 to 0.0657 between rice varieties, 0.0124 to 0.0207 with ABS, and 0.0321 to 0.0499 with bristle brushes. After whitening treatment, these coefficients increased to 0.0490 to 0.0751, 0.0168 to 0.0286, and 0.0411 to 0.0657, respectively. Higher moisture content elevates these coefficients, reducing flowability. The order of dynamic friction coefficients, from highest to lowest, was: rice seeds, bristle brushes, and ABS material. This indicates that rice seeds flow most easily over ABS surfaces, but exhibit greater resistance when interacting with other seeds. These findings provide important insights for future structural design considerations.

***Elastic Modulus***

After each sample test, the pressure versus displacement curve was exported using software compatible with the testing machine. Stable data before the yield point was selected, and stress and strain values were calculated to determine the elastic modulus, as shown in Table 3. Differences in the elastic modulus were observed at varying moisture contents. As moisture content increased, the elastic modulus decreased, as higher moisture reduced cohesion between seeds, leading to decreased stiffness. In dry conditions, the elastic modulus ranged from 365.27 to 418.19 MPa, while chitting treatment reduced it to 180.92 to 209.15 MPa.

**Table 3**

**Elastic modulus test results**

| Experiment Rice Seeds | Elastic Modulus/MPa | Experiment Rice Seeds | Elastic Modulus/MPa |
|---|---|---|---|
| $G_1$-$M_1$ | 365.27 | $G_2$-$M_1$ | 206.37 |
| $G_1$-$M_2$ | 371.96 | $G_2$-$M_2$ | 194.12 |
| $G_1$-$M_3$ | 379.60 | $G_2$-$M_3$ | 200.35 |
| $G_1$-$M_4$ | 377.72 | $G_2$-$M_4$ | 209.15 |
| $G_1$-$M_5$ | 388.63 | $G_2$-$M_5$ | 192.56 |
| $G_1$-$M_6$ | 398.74 | $G_2$-$M_6$ | 183.01 |
| $G_1$-$M_7$ | 376.26 | $G_2$-$M_7$ | 204.54 |
| $G_1$-$M_8$ | 410.45 | $G_2$-$M_8$ | 184.49 |
| $G_1$-$M_9$ | 407.03 | $G_2$-$M_9$ | 180.92 |
| $G_1$-$M_{10}$ | 418.19 | $G_2$-$M_{10}$ | 184.70 |

***Shear Modulus***

During the shear modulus testing process, the same experimental method as the elastic modulus was used to process the data of the samples to obtain the shear modulus of the samples, and the test results were shown in Table 4. The analysis of the results revealed that there were differences in the shear modulus of rice seeds at different moisture contents. With an increase in moisture content of each rice seed, the shear modulus of the test sample showed a decreasing trend. When rice seeds are in dry condition, the shear modulus ranged from 137.38 to 151.88 MPa. When rice seeds underwent chitting treatment, the shear modulus ranged from 74.08 to 82.45 MPa.

**Table 4**

**Shear modulus test results**

| Experiment Rice Seeds | Shear Modulus/MPa | Experiment Rice Seeds | Shear Modulus/MPa |
|---|---|---|---|
| $G_1$-$M_1$ | 137.38 | $G_2$-$M_1$ | 81.58 |
| $G_1$-$M_2$ | 139.27 | $G_2$-$M_2$ | 77.69 |
| $G_1$-$M_3$ | 141.51 | $G_2$-$M_3$ | 79.76 |
| $G_1$-$M_4$ | 140.89 | $G_2$-$M_4$ | 82.45 |
| $G_1$-$M_5$ | 144.00 | $G_2$-$M_5$ | 77.19 |
| $G_1$-$M_6$ | 146.77 | $G_2$-$M_6$ | 74.08 |
| $G_1$-$M_7$ | 140.48 | $G_2$-$M_7$ | 80.85 |
| $G_1$-$M_8$ | 149.83 | $G_2$-$M_8$ | 74.49 |
| $G_1$-$M_9$ | 148.91 | $G_2$-$M_9$ | 73.46 |
| $G_1$-$M_{10}$ | 151.88 | $G_2$-$M_{10}$ | 74.63 |

***Impact Restitution Coefficient Test Results and Analysis***

The test results for the impact restitution coefficient, as outlined in Table 5, indicated a positive correlation between the moisture content of rice seeds and their deformation upon collision.

Higher moisture content resulted in increased deformation, led to greater energy loss during impact, thus reduced the normal separation velocity and subsequently the impact restitution coefficient. In dry conditions, the impact restitution coefficient ranged from 0.412 to 0.471 between rice seeds, 0.438 to 0.501 between rice seeds and ABS material, and 0.454 to 0.519 between rice seeds and brush. After chitting treatment, these values decreased to 0.351 to 0.408, 0.357 to 0.414, and 0.396 to 0.460, respectively. The coefficients were ranked from highest to lowest as follows: rice seeds and brush, rice seeds and rice seeds, and rice seeds and ABS material, across both states of the rice seeds.

**Table 5**

**Experimental results of collision recovery coefficient**

| Experiment Rice Seeds | Impact Contact Materials | | | Experiment Rice Seeds | Impact Contact Materials | | |
|---|---|---|---|---|---|---|---|
| | Rice Seeds | ABS | Brushes | | Rice Seeds | ABS | Brushes |
| $G_1$-$M_1$ | 0.412 | 0.438 | 0.454 | $G_2$-$M_1$ | 0.402 | 0.362 | 0.454 |
| $G_1$-$M_2$ | 0.419 | 0.446 | 0.462 | $G_2$-$M_2$ | 0.379 | 0.384 | 0.427 |
| $G_1$-$M_3$ | 0.427 | 0.454 | 0.470 | $G_2$-$M_3$ | 0.389 | 0.374 | 0.438 |
| $G_1$-$M_4$ | 0.426 | 0.453 | 0.469 | $G_2$-$M_4$ | 0.408 | 0.357 | 0.460 |
| $G_1$-$M_5$ | 0.437 | 0.465 | 0.481 | $G_2$-$M_5$ | 0.376 | 0.387 | 0.424 |
| $G_1$-$M_6$ | 0.448 | 0.477 | 0.494 | $G_2$-$M_6$ | 0.357 | 0.407 | 0.403 |
| $G_1$-$M_7$ | 0.424 | 0.452 | 0.467 | $G_2$-$M_7$ | 0.403 | 0.361 | 0.454 |
| $G_1$-$M_8$ | 0.462 | 0.492 | 0.509 | $G_2$-$M_8$ | 0.362 | 0.402 | 0.408 |
| $G_1$-$M_9$ | 0.459 | 0.488 | 0.505 | $G_2$-$M_9$ | 0.351 | 0.414 | 0.396 |
| $G_1$-$M_{10}$ | 0.471 | 0.501 | 0.519 | $G_2$-$M_{10}$ | 0.361 | 0.403 | 0.407 |

### *External Load and Survival Characteristics Test Results and Analysis*

After the external load and survival characteristics test method, static loads ranged from 0N to 50N were applied to the test samples. The resulting data was used to plot a load-survival rate curve, as shown in Fig. 7.

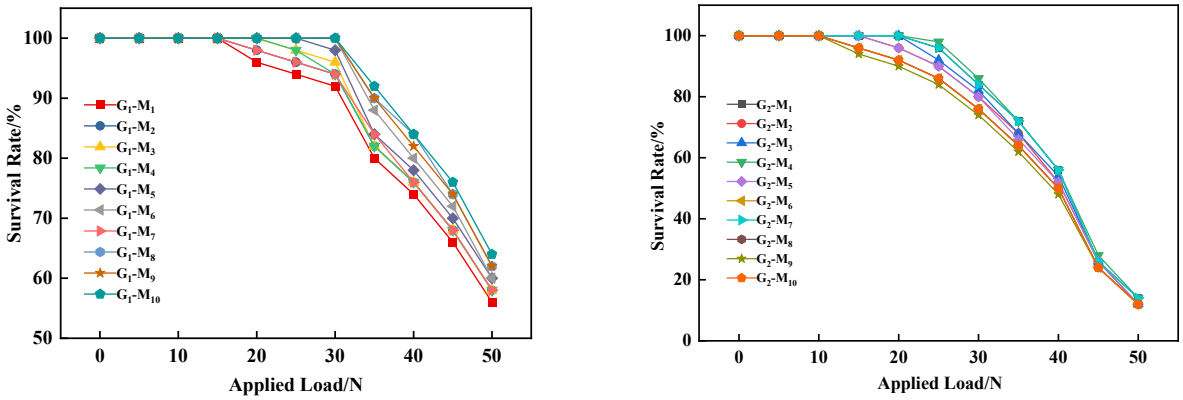


(a) (b)

**Fig. 7 - Survival rate and applied load curve of rice seeds**

*(a) Dry Rice Seeds (b) Chitting Treatment*

Analysis revealed a decline in the survival rate of rice seeds with increased static load. For the same type of seeds, higher moisture content correlated with a reduced ability to withstand static loads, making them more susceptible to breakage. In dry conditions, survival rates ranged from 62% to 100%, but rapidly dropped below 90% when loads exceeded 35N. For seeds undergoing chitting treatment, survival rates ranged from 12% to 100%, with a noticeable declined when loads exceeded 20N, and a rapid dropped below 90% beyond 25N. Further analysis indicated that excessive static loads compromised seed survival by rupturing the surface membrane, disrupting moisture regulation, and impairing germination and growth. The data showed that external loads up to 20N did not significantly impact germination, with survival rates remaining above 92%. These findings suggest that, during direct seeding, rice seeds can withstand certain levels of external load without compromising viability.

### *Cutting and Seedling Characteristics*

Using the experimental method for cutting and seedling characteristics, cuts were made along the embryo axis of rice seeds at lengths from 0 mm to 3 mm. A relationship curve between cutting length and survival rate was plotted, as shown in Figure 8.

The results indicated that survival rates decreased with increased cutting length, underscored the critical impact of embryo damage on seed survival. In dry conditions, survival rates ranged from 48% to 100%, with a rapid decline beyond 1.5 mm. For seeds undergoing chitting treatment, survival rates ranged from 38% to 100%, with a noticeable drop below 90% when the cutting depth exceeded 1.0 mm. Further analysis showed that seeds with larger three-axis dimensions exhibited slightly higher survival rates under the same cutting length. Additionally, higher moisture content enabled seeds to maintain survival rates above 90% when cutting lengths did not exceed 1.5 mm. These findings suggest that during direct seeding, minor damage to seeds does not significantly impact survival, provided that the cutting depth remains within these thresholds.

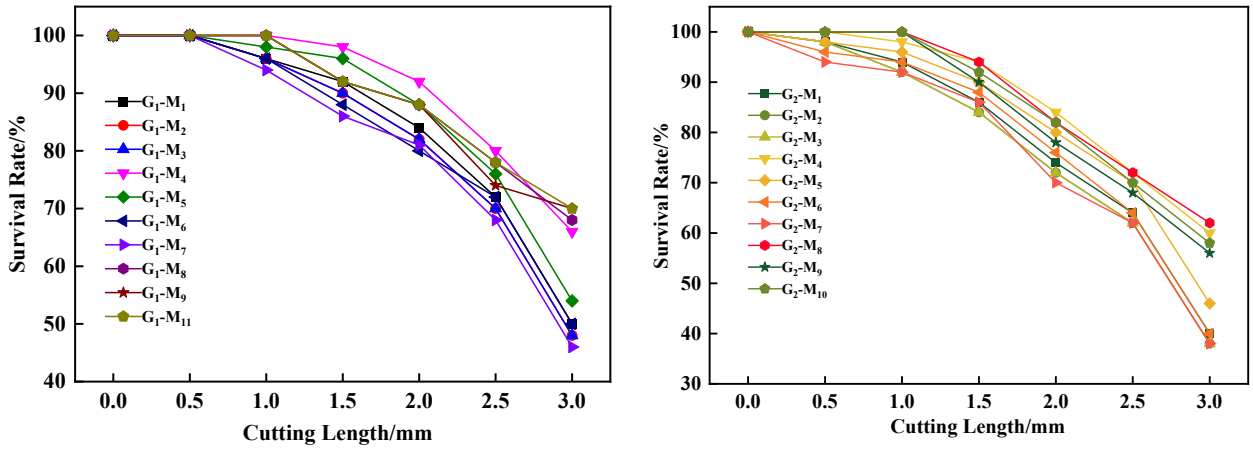


(a) (b)

**Fig. 8 - Survival rate and cut length curve of rice seeds**

*(a) Dry Rice Seeds (b) Chitting Treatment*

## CONCLUSIONS

The study's methodology and results offered a robust theoretical foundation and data support for optimizing planter design, constructing theoretical models for various processes, and conducting virtual simulations. The main conclusions were as follows.

For untreated rice seeds, static friction coefficients with seeds, ABS plastic, and bristle plates ranged from 0.31-0.41, 0.20-0.30, and 0.24-0.34, respectively, with dynamic coefficients at 0.0411-0.0657, 0.0124-0.0207, and 0.0321-0.0499. Post-chitting, static coefficients increased to 0.52-0.64, 0.37-0.48, and 0.41-0.52, with dynamic coefficients at 0.0490-0.0751, 0.0168-0.0286, and 0.0411-0.0657.

For untreated seeds, the restitution coefficients with seeds, ABS plastic, and bristle plates were 0.412-0.471, 0.438-0.501, and 0.454-0.519. After chitting, these stabilized at 0.351-0.408, 0.357-0.414, and 0.396-0.460, respectively. Untreated seeds showed an elastic modulus of 365.27-418.19 MPa, shear modulus of 137.38-151.88 MPa. Chitting reduced these values to 180.92-209.15 MPa, 74.08-82.45 MPa.

Under dry conditions, maintaining an external load below 20 N and a cutting length under 1.5 mm ensured seed survival rates above 90%. While this study provided a comprehensive analysis of the frictional and mechanical properties of rice seeds, it did not include calibration experiments for key parameters, which represents a noted limitation of the research.

## ACKNOWLEDGEMENT

We are grateful to the Henan Provincial Science and Technology Attack Project/Henan Nanyang Municipal Science and Technology Attack Project for its financial support under grant number 252102111175/2024KJGG0102. We also extend special thanks to the National Engineering Research Center for Agricultural Intelligent Equipment for its contributions to this research.

## REFERENCES

[1] Baral, B.R., Pande, K.R., Gaihre, Y.K., Baral, K.R., Sah, S.K., Thapa, Y.B., and Singh, U. (2021). Real-time nitrogen management using decision support-tools increases nitrogen use efficiency of rice. *Nutrient Cycling in Agroecosystems,* 119, 355-368.

[2] Dong, H., Zhang, B., Jiang, T., Zhang, Y., Qu, J., Chen, C., Xiao, Y., Ding, Y., Xi, X. (2022). Design and Optimization of Rice Grain Screening System Based on DEM–CFD Coupled Rice Seed Testing Platform. *Agronomy-Basel,* 12(12), 3069.

[3] Dun, G., Mao, N., Gao, Z., Wu, X., Liu, W., Zhou, C. (2022). Model construction of soybean average diameter and hole parameters of seed-metering wheel based on DEM. *International Journal of Agricultural and Biological Engineering*, 15, 101-110.
[4] Gao, X., Zhao, P., Li, J., Xu, Y., Huang, Y., Wang, L. (2022). Design and Experiment of Quantitative Seed Feeding Wheel of Air-Assisted High-Speed Precision Seed Metering Device. *Agriculture-Basel,* 12(11), 1951.
[5] He, S., Qian, C., Jiang, Y., Qin, W., Huang, Z., Huang, D., Wang, Z., Zang, Y. (2024). Design and optimization of the seed feeding device with DEM-CFD coupling approach for rice and wheat. *Computers and Electronics in Agriculture,* 219, 108814.
[6] He, S., Zang, Y., Huang, Z., Tao, W., Xing, H., Qin, W., Jiang, Y., Wang, Z. (2022). Design of and Experiment on a Cleaning Mechanism of the Pneumatic Single Seed Metering Device for Coated Hybrid Rice. *Agriculture-Basel*, 12(8), 1239.
[7] Li, H., Ling, L., Wen, C., Liu, H., Wu, G., An, X., Meng, Z., Yan, B. (2023a). Structural optimization method of rice precision direct seed-metering device based on multi-index orthogonal experimental. *Frontiers in Plant Science,* 14, 1183624.
[8] Li, H., Yan, B., Meng, Z., Ling, L., Yin, Y., Zhang, A., Zhao, C., Wu, G. (2023b). Study on influencing factors of hole-filling performance of rice precision direct seed-metering device with hole ejection. *Biosystems Engineering,* 233, 76-92.
[9] Li, H., Zhao, C., Yan, B., Ling, L., Meng, Z. (2022). Design and Verification of the Variable Capacity Roller-Wheel Precision Rice Direct Seed-Metering Device. *Agronomy-Basel*, 12(8), 1798.
[10] Li, J., Lai, Q., Zhang, H., Zhang, Z., Zhao, J., Wang, T. (2021). Suction force on high-sphericity seeds in an air-suction seed-metering device. *Biosystems Engineering*, 211, 125-140.
[11] Liberatore, C.M., Biancucci, M., Ezquer, I., Gregis, V., Di Marzo, M. (2025). Investigating how reproductive traits in rice respond to abiotic stress. Journal of Experimental Botany. https://doi.org/10.1093/jxb/eraf031
[12] Liu, W., Zhou, Z., Xu, X., Gu, Q., Zou, S., He, W., Luo, X., Huang, J., Lin, J., Jiang, R. (2023). Evaluation method of rowing performance and its optimization for UAV-based shot seeding device on rice sowing. *Computers and Electronics in Agriculture,* 207, 107718.
[13] Qian, C., He, S., Qin, W., Jiang, Y., Huang, Z., Zhang, M., Zhang, M., Yang, W., Zang, Y. (2024). Influence of Shaped Hole and Seed Disturbance on the Precision of Bunch Planting with the Double-Hole Rice Vacuum Seed Meter. *Agronomy-Basel*, 14(4), 768.
[14] Shang, Y., Zhou, B., Yang, J., Zhang, S. (2024). Design and experiment of impeller seed guide device for rice internal suction hole direct seeding device. *Scientific Reports*, 14, 63-71.
[15] Shun, Z., Yong, L., Haoyu, W., Juan, L., Zhaodong, L., Dequan, Z. (2020). Design and Experiment of U-shaped Cavity Type Precision Hill-drop Seed-metering Device for Rice. Nongye Jixie Xuebao. *Transactions of the Chinese Society of Agricultural Machinery*, 51(10), 98-108.
[16] Tang, H., Jiang, Y., Xu, C., Zhou, W., Wang, Q., Wang, Y. (2021). Experimental study on the correlation between hill direct seeding rate and field seedling rate of typical rice varieties in cold areas. *International Journal of Agricultural and Biological Engineering,* 14, 63-71.
[17] Wang, B., Na, Y., Pan, Y., Ge, Z., Liu, J., Luo, X. (2022a). CFD Simulation and Experiments of Pneumatic Centralized Cylinder Metering Device Cavity and Airflow Distributor. *Agronomy-Basel*, 12(8), 1775.
[18] Wang, J., Xu, C., Qi, X., Zhou, W., Tang, H. (2022b). Discrete Element Simulation Study of the Accumulation Characteristics for Rice Seeds with Different Moisture Content. *Foods*, 11(3),295.
[19] Xing, H., Wang, Z., Luo, X., Zang, Y., He, S., Xu, P., Liu, S. (2021). Design and experimental analysis of rice pneumatic seeder with adjustable seeding rate. *International Journal of Agricultural and Biological Engineering*, 14, 113-122.
[20] Xing, H., Wang, Z., Luo, X., Zang, Y., Yang, W., Zhang, M., Ma, Y. (2018). Design of an active seed throwing and cleaning unit for pneumatic rice seed metering device. *International Journal of Agricultural and Biological Engineering*, 11, 62-69.
[21] Xing, H., Zang, Y., Wang, M.Z., Luo, W.X., Zhang, H.M., Fang, Y.L. (2020). Design and experimental analysis of a stirring device for a pneumatic precision rice seed metering device. *Transactions of the Asabe*, 63, 799-808.
[22] Zhang, M., Wang, Z., Luo, X., Zang, Y., Yang, W., Xing, H., Wang, B., and Dai, Y. (2018). Review of precision rice hill-drop drilling technology and machine for paddy. *International Journal of Agricultural and Biological Engineering*, 11, 1-11.